

## SUPPLEMENTARY INFORMATION

### Membrane targeting of mGluR1 and GluD2 in HEK cells (Figures S1-S3)

In order to verify correct membrane targeting, we expressed mGluR1-YFP, GluD2 and GluD2 V617R in HEK93 cells and examined their respective localization by immunofluorescence using antibodies against YFP and the C terminal tail of GluD2. All proteins were localized at the membrane in all tested combinations (mGluR1-YFP, GluD2, mGluR1-YFP+GluD2 and mGluR1-YFP+GluD2V617R, figure S1-S3).

### SUPPLEMENTARY METHODS

**Plasmids and virus production** - GluD2 coding sequence was obtained by PCR from cerebellar cDNA using Pfu turbo (Stratagene, La Jolla, CA). 5' and 3' overlapping fragments were amplified separately and then assembled in pcDNA3.0 (Invitrogen, Carlsbad, CA) between KpnI and NotI sites using the unique internal BstXI site. mGlu1, NR1A and NR1B sequences are derived from the rat (*Rattus norvegicus*). The mGlu1-YFP tagged receptor was used in HEK293 cells, the complete description is provided in [1]. The YFP-sequence was inserted upstream the coding sequence of mGluR1 to select HEK293 cells that co-express mGlu1. In some experiments, an untagged mGlu1 was also used, no difference was detectable with the mGlu1-YFP.

The V617R mutation was introduced into GluD2 coding sequence using the QuikChange II XL kit (Agilent technologies, Massy, France).

**HEK293 cell culture and transfection** - HEK293 cells were transfected with the plasmids of interest depending on the experiments (mGlu1, mGlu1-YFP, NR1, NR2A, GluD2 and/or GluD2V617R) plus a plasmid encoding GFP in equal proportion and

the cells were selected based on YFP and/or GFP fluorescence. For experiments using the recombinant virus, cells were selected based on GFP fluorescence given that the viral construct has a GFP coding sequence.

**Electrophysiology** – In HEK293 cells, whole-cell currents were acquired with the patch-clamp technique in whole cell configuration at -70 mV using an Axopatch 200B amplifier (Axon Instrument, Molecular Devices, Sunnyvale, CA). The signal was digitized at 3 kHz and filtered at 1 kHz. Average peak current amplitudes were estimated using the pClamp9 (Molecular Devices) software. Internal medium contained (in mM): 140 CsCl, 0.5 CaCl<sub>2</sub>, 20 EGTA, 10 HEPES, 10 D-glucose, pH 7.2 and osmolarity of 300 mOsm. External medium contained (in mM): 140 NaCl, 2 CaCl<sub>2</sub>, 3 KCl, 10 HEPES, 10 D-glucose, 0.01 glycine, 0.0003 tetrodotoxin, pH 7.4 and osmolarity of 330 mOsm.

For Purkinje cell recordings, animals were first anesthetized with halothane and then rapidly decapitated. The cerebellar vermis was immediately removed and cooled down to 4°C in oxygenated bicarbonate buffered solution (BBS) (see below). Parasagittal 180 µm thick slices were cut with a vibratome (VT-1000S; Leica, Wetzlar, Germany). Slices were incubated for at least 1 h at room temperature (RT) in the BBS before any recording. The external medium BBS contained (in mM): 130 NaCl, 2.5 KCl, 2.0 CaCl<sub>2</sub>, 1.0 MgCl<sub>2</sub>, 26.0 NaHCO<sub>3</sub>, 1.3 NaH<sub>2</sub>PO<sub>4</sub>, and 10.0 glucose, pH 7.4 when bubbled with 95%O<sub>2</sub> and 5% CO<sub>2</sub>. We worked at room temperature (approx 25° C). BBS was applied with a gravity driven perfusion system at an averaged speed of 1.5 ml/min. The patch pipettes had a resistance of 2-4 MΩ when filled with the following solution (in mM): 144.0 K gluconate, 6.0 KCl, 4.6 MgCl<sub>2</sub>, 10.0 HEPES acid, 1.0 EGTA 0.1 CaCl<sub>2</sub>, 4.0 ATP-Na, 0.4 GTP-Na, pH 7.3 adjusted with KOH. In Purkinje cells DHPG currents were acquired in the presence of TTX,

bicuculline, NBQX and D-APV (resp. 1, 20, 10, 50  $\mu$ M). PF-slowEPSCs were recorded in the presence of bicuculline, NBQX and D-APV (resp. 10, 10, 50  $\mu$ M).

**Stimulation protocol to induce PF-slow EPSCs :** Tetanic stimulation of PFs are required to recruit mGlu1 that locate at the periphery of synapses. Thus, the synaptic stimulation of mGlu1 were performed as following: Each PFs burst used to activate mGlu1s consisted in 8 constant-voltage pulses, of 1 ms duration each, repeated at 100 Hz and delivered through a monopolar patch-like pipette filled with BBS. These [8 X 100 Hz] trains were repeated at no more than 1 minute intervals to avoid rundown of the mGlu1 slow EPSC. If the stimulation train was repeated more frequently, for example every 10 sec, the mGlu1 slow EPSC rapidly decreases down to 60 pA amplitude on average, where it maintains for the rest of the recording. This may constitute a major difference between our study and others, but this is hardly verifiable, as this frequency is rarely indicated in the publications. Since GluD2s locate at PFs but not at climbing fiber synapses in the adult, we also took care not to recruit the climbing fibers, as assessed by paired-pulse facilitation of the response before adding NBQX and D-APV (supplementary figure S4). This is particularly important in the HO-Nancy Purkinje cells that display multiple-innervation by the climbing fibers even at the adult stage [5].

**Calibration of the mGluR1-dependent PF-slow EPSC -** In Hotfoot mutants, half of the PFs synapses is absent or abnormal (“synaptic mismatch” see [5]). Thus, in order to recruit comparable PFs input in WT and HO-Nancy Purkinje cells, it was necessary to calibrate the PF-mediated response (supplementary figure). This was done as following: After the whole-cell recording was achieved, we switched to current-clamp mode and the intensity of PFs stimulation was set at the threshold of discharge of one spike (i.e. half of the stimulations mediating a spike, supplementary

figure S4). We verified that the corresponding PF-EPSCs obtained in voltage-clamp with this calibration method had similar amplitudes in WT and HO-Nancy Purkinje cells, which was the case (supplementary figure S4). This indicates that, despite the abnormalities described at PFs synapses, the input/output response of the functional PFs input of HO-Nancy Purkinje cells remained quantitatively comparable to that of WT animals. Given that the number of mGlu1s does not seem to significantly change in GluD2 knock-out mice, it seems reasonable to consider that our calibrated stimulations recruit roughly comparable amount of mGlu1s from cell to cell in the WT or mutant mice.

**Drugs** - NBQX: 2,3-dihydroxy-6-nitro-7-sulfamoyl-benzo[f]quinoxaline-2,3-dione; D-APV: D-(-)-2-Amino-5-phosphonopentanoic acid; NASPM: N-[3-[[4-[(3-Aminopropyl)amino]butyl]amino]propyl]-1-naphthaleneacetamide trihydrochloride; AIDA: (RS)-1-Aminoindan-1,5-dicarboxylic acid; Pyr3: Ethyl-1-(4-(2,3,3-trichloroacrylamide)phenyl)-5-(trifluoromethyl)-1H-pyrazole-4-carboxylate. Drugs were applied in the bath for all the experiments. In all the cases, we verified that the application, in the same conditions, of a control solution without the drugs but with the vehicle did not have any detectable effect. For HEK293 cells experiments, either the racemate (R,S)- or the active enantiomer (S)-DHPG were used at 100 $\mu$ M, both producing undistinguishable effects. For this reason, the data obtained with both forms were pooled. (S)-DHPG (50 $\mu$ M) was always used for acute slices experiments.

**Immunohistochemistry, equipment and settings** - The cerebellar vermis was cut into 60  $\mu$ m parasagittal slices. The free-floating slices were rinsed three times in phosphate buffered saline (PBS) before 1h permeabilization and saturation with PBS containing 0.25% Triton-X, 0.2% gelatin, 0.1% sodium azide and lysine (0.1 M) before applying overnight primary antibody. Anti-GluD2 and anti-GluD1/2 were rabbit

polyclonal antibodies. Anti-calbindin antibody was a mouse monoclonal antibody. Anti-rabbit CY3 (1/200; Jackson ImmunoResearch Laboratories) and goat anti-mouse alexa fluor 488 (1/400, Invitrogen) were used to reveal GluD2 and the Purkinje cell marker Calbindin labeling respectively. The labelled slices were mounted in Mowiol. In multiple-labelling experiments, acquisition of the signal was systematically performed in sequential mode. Images of GluD2 immunolabelings (Fig. 3B) were taken in the lobule V of the vermis using a Leica SP5 confocal microscope. Images of GluD1/2 (in supplementary fig. S5) were acquired with Zeiss LSM510 and LSM710 microscopes. The 16-bit confocal images were acquired with 40x and 63x objectives, a frame size of 1024 x 1024 pixels and processed with the ImageJ software (public domain: <http://rsbweb.nih.gov/ij/>).

**Injection of the viruses** - Two months old C57BL/6 mice were anesthetized -ip injection- with ketamine (146 mg/Kg) and xylazine (7.4 mg/Kg) and placed on a Kopf stereotaxic apparatus (Harvard Apparatus). One injection of viruses (2  $\mu$ l, over 8 min) was performed per animal on the midline at the suture between the parietal and the occipital bones, and 0.5 mm from pial surface to hit lobule VI of the vermis. 3 animals received the virus carrying the dominant negative GluD2 and 3 received the control virus expressing GFP alone. The animals were killed 24 or 48 hours after injection to perform acute electrophysiological studies.

**Animals** – Mice (*Mus musculus*) of either gender were used, aged between 8 weeks and 6 months (average 14.3 weeks), either for immunohistochemistry or electrophysiology. Animal breeding and euthanasia were performed by authorized people (NOR ATEN0090478A) in accordance to European and French legislation at the moment of the experiments (code rural art. 276). Animal welfare and prevention of suffering was a constant preoccupation, any experiment being discarded in case of

any suffering sign. HO-Nancy mice are on the C57BL/6 genetic background and have been previously described [4, 5]; they are raised at the C. Levenes lab. Wildtype mice were purchased at Janvier Laboratory (Le Genest-St-Isle, France).

**Membrane targeting of mGluR1-YFP, GluD2 and GluD2 V617R** - Twenty four hours after transfection, HEK cells were fixed for 20 min at room temperature with 4% paraformaldehyde in PBS and then washed several times in PBS. Next, cells were blocked and permeabilized by incubating them with a PBS/Gelatine 0.2%/Triton X-100 0.3% (PBS-GT) solution before 2h incubation at 4°C with primary antibodies diluted in PBS-GT. After several washes in PBS-GT, cells were incubated for 1h at room temperature with secondary antibodies diluted in PBS-GT. After several washes in PBS, cells were mounted in Prolong gold (Life technologies). Antibodies were used as follows: rabbit anti GluD2C (1:1000, Frontiers sciences, Japan), chicken anti-GFP (1:1000, Aves labs, this antibody recognize also YFP), alexafluor 488-conjugated goat anti-chicken IgG (1:2000, Life technologies, UK) and alexafluor 555-conjugated goat anti-rabbit IgG (1:2000, Life technologies, UK). Fluorescence images were acquired using a TCS SPE confocal microscope (Leica, Germany) using an x63 objective.

**Number of cells/experiments** - In the main text, “n” represents the number of cells taken into account for the statistics. The selection of the cells to be discarded was based only on the quality of the recordings (input resistance, series resistance, leak current, stability of the recording). For each experiments in HEK cells, at least 7 different cells derived from at least 3 different cultures were used. For experiments made in slices, the number of independent cells used for the statistics is indicated in

the main text and/or in the figure, at least 3 independent experiments (i.e. 3 different mice) were required to draw any conclusion.

In case of the drug tests (for example D-serine, NASPM etc.), controls and tests were performed on the same cell to take into account the variation of the transfection efficacy from cell to cell in case of the cultures, and to take into account the cell-to-cell or animal-to-animal variability in the case of cerebellar slices. Accordingly, paired statistics were used in these cases.

## **SUPPLEMENTARY FIGURES LEGENDS**

**Figure S1- Correct membrane targeting of mGluR1 and GluD2 expressed separately (alone) in HEK cells.** Confocal section of 3 different fields containing HEK cells expressing either mGluR1-YFP (left) or GluD2 (right) and immunolabeled against YFP (green) and GluD2 (red) respectively. Scale bar 20  $\mu$ m.

**Figure S2- Correct membrane targeting of coexpressed mGluR1 and GluD2 in HEK cells.** Confocal section of 3 different fields containing HEK cells expressing both mGluR1-YFP and GluD2 and immunolabeled against YFP (1st column) and GluD2 (2nd column) respectively. Scale bar 20  $\mu$ m.

**Figure S3- Correct membrane targeting of coexpressed mGluR1 and GluD2 V617R in HEK cells.** Confocal section of 3 different fields containing HEK cells expressing both mGluR1-YFP and GluD2 V617R and immunolabeled against YFP (1st column) and GluD2 (2nd column) respectively. Scale bar 20  $\mu$ m.

**Figure S4- Calibration of the mGluR1-dependent PF-slow EPSC- A)** Repetitive stimulation of PF (8 pulses at 100 Hz) induced in WT Purkinje cells a slow EPSC that depended on mGlu1 receptors activation. Application of the group I mGluR antagonist AIDA completely blocked PF-slow EPSC. Traces were recorded at -70

mV and in the presence of bicuculline, NBQX and D-APV. Note that the kinetics of the slow PF-EPSCs illustrated here is slower than the rest of the PF-slow EPSCs illustrated in this study, except figure 2E. In our hands, these kinetics were variable from cell to cell, whatever the genotype or manipulation. They did not result from any manipulation of GluD2 or from side effects of the viral transduction methods. This was true for WT, as shown in this figure, for HO-Nancy mice, and also for Purkinje cells transduced with Sinbis viruses, whatever the constructs used. We could not make any correlation between these kinetics and, for example, the amplitude of the initial AMPA mediated PF-EPSC (before we add NBQX), the effects of Pyr3, or the position of the stimulating pipette. We have no explanation for this cell-to-cell variability. By contrast, fig. 2B and 2C, show example of individual PF-slow EPSCs recorded from 2 different cells with faster kinetics. Such cells are more representative of the kinetics we generally encountered in our experiments. **B)** In Hotfoot mutants, half of the PFs synapses are absent or abnormal. In order to recruit comparable amount of functional synapses in WT and HO-Nancy mice, it was necessary to calibrate the PF-mediated response. PF stimulation intensity was set at the threshold of discharge of one spike (left traces). The spikes had the same shape in WT and HO cells. The amplitude of PF-mediated EPSCs recorded with this calibration method had similar amplitudes in WT and HO-Nancy Purkinje cells (histogram). **C)** Example of a PF-slow EPSC in HO-Nancy. In this example of an HO-Nancy Purkinje cell, the fast component of the PF-mediated EPSC totally disappeared in the presence of NBQX and D-APV (bottom traces). Note that the mGluR1-mediated slow EPSC was totally absent despite the recruitment of a substantial number of PFs as visible before NBQX and D-APV.

**Figure S5- Immunolabeling of cerebellar slices done with anti-GluD1/2 and anti-CALB1 antibodies.** Confocal images of calbindin (CALB1, red) and GluD1/2 (green) immunolabelings, in WT (top) and HO-Nancy mice (bottom). Scale bars, 20 microm

## SUPPLEMENTARY REFERENCES

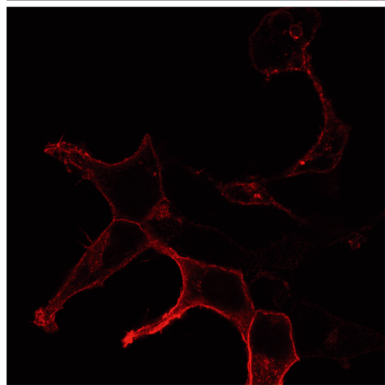
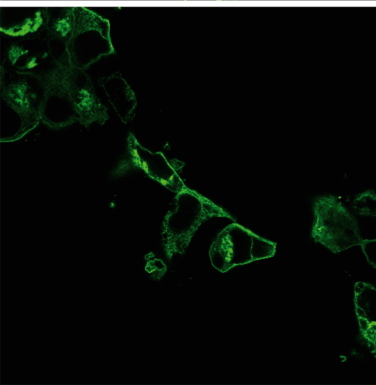
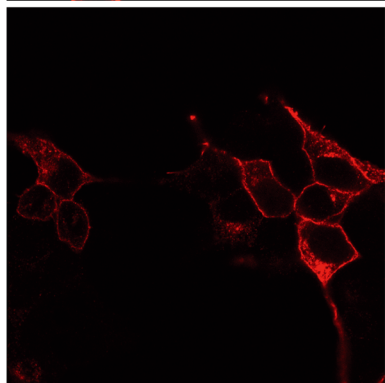
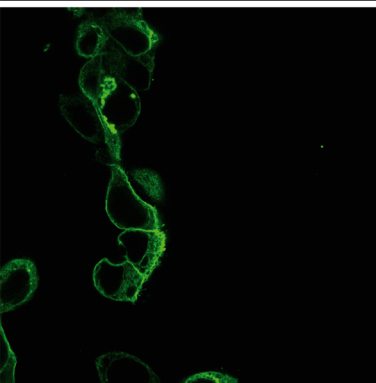
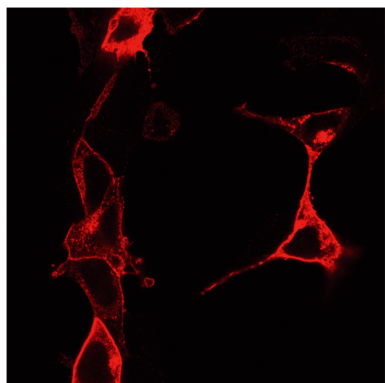
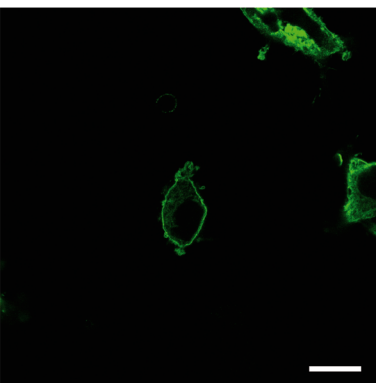
1. Perroy J, Raynaud F, Homburger V, Rousset MC, Telley L, Bockaert J, Fagni L (2008) Direct interaction enables cross-talk between ionotropic and group I metabotropic glutamate receptors. *J Biol Chem* 283: 6799-6805
2. Okada T, Yamada N, Kakegawa W, Tsuzuki K, Kawamura M, Nawa H, Iino M, Ozawa S (2001) Sindbis viral-mediated expression of Ca<sup>2+</sup>-permeable AMPA receptors at hippocampal CA1 synapses and induction of NMDA receptor-independent long-term potentiation. *Eur J Neurosci* 13: 1635-1643
3. Piochon C, Irinopoulou T, Bruscianno D, Bailly Y, Mariani J, Levenes C (2007) NMDA receptor contribution to the climbing fiber response in the adult mouse Purkinje cell. *J Neurosci* 27: 10797-10809
4. Guastavino JM, Sotelo C, Damez-Kinselle I (1990) Hot-foot murine mutation: behavioral effects and neuroanatomical alterations. *Brain Res* 523: 199-210.
5. Lalouette A, Lohof A, Sotelo C, Guenet J, Mariani J (2001) Neurobiological effects of a null mutation depend on genetic context: comparison between two hotfoot alleles of the delta-2 ionotropic glutamate receptor. *Neuroscience* 105: 443-455.

HEK/mGluR1-YFP

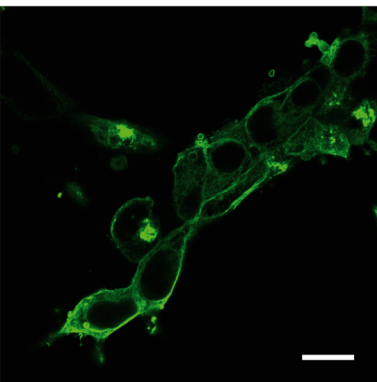
HEK/GluD2

Anti YFP

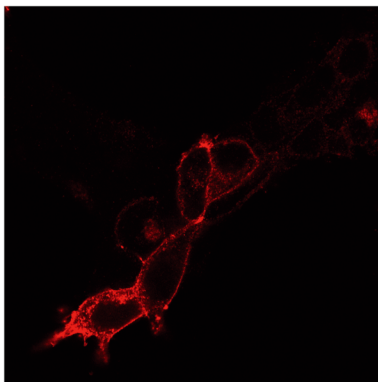
Anti GluD2



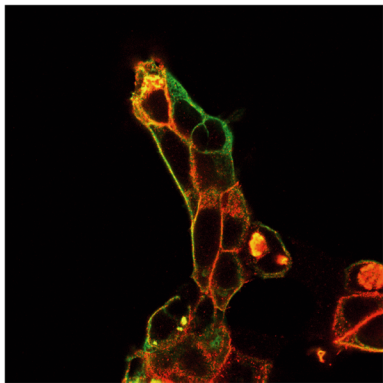
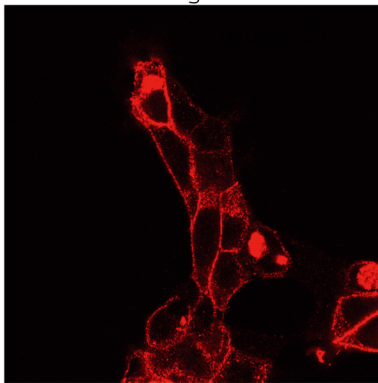
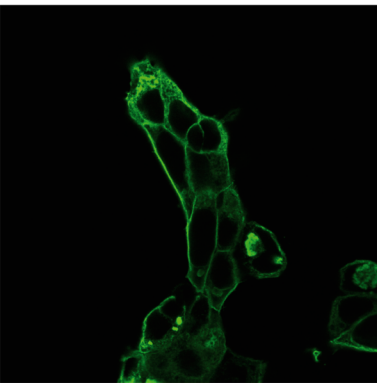
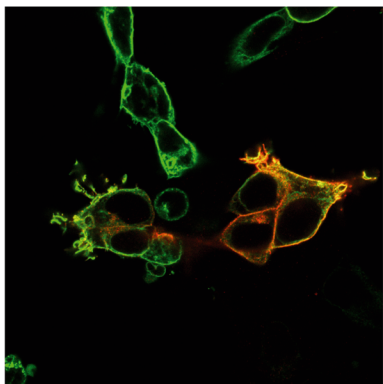
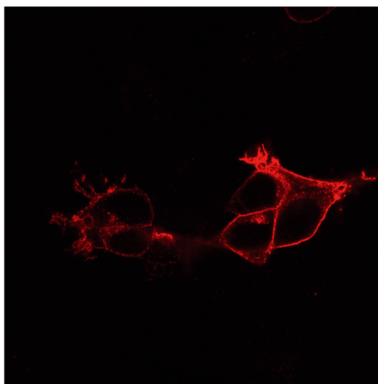
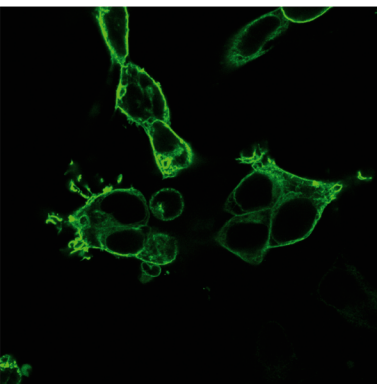
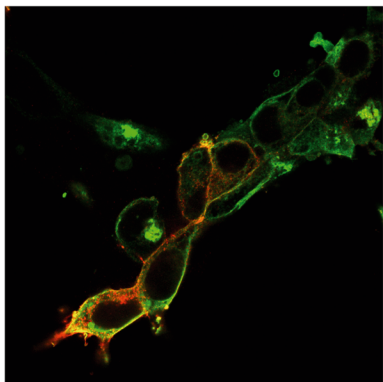
Anti YFP



Anti GluD2



Merge



HEK/mGluR1-YFP+GluD2

Anti YFP

Anti GluD2

Merge

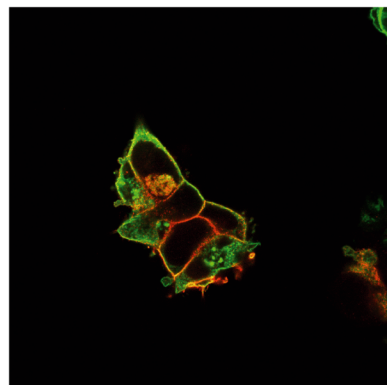
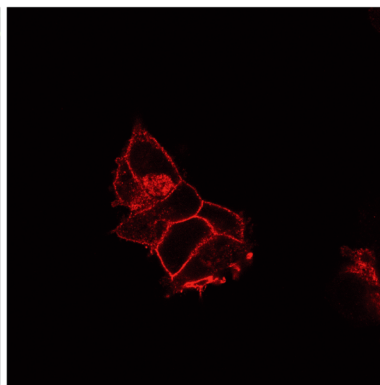
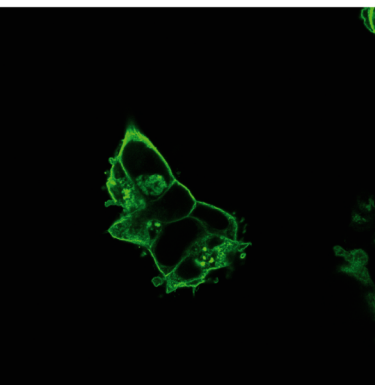
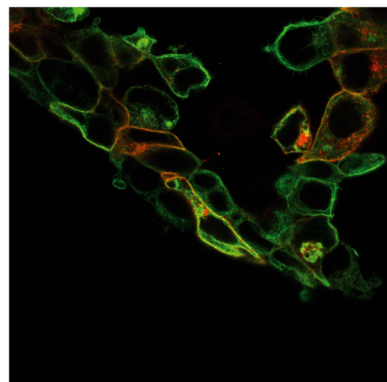
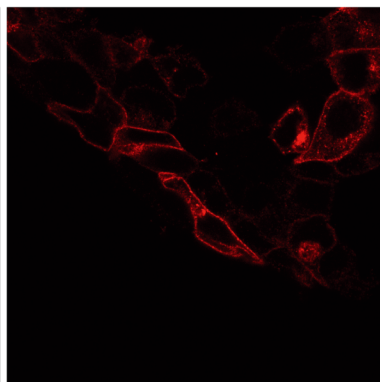
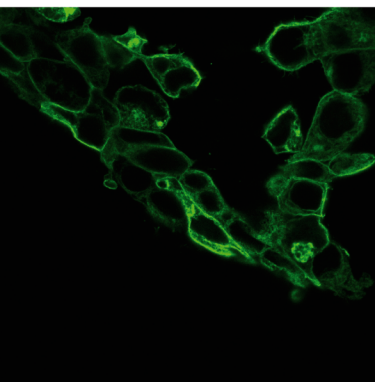
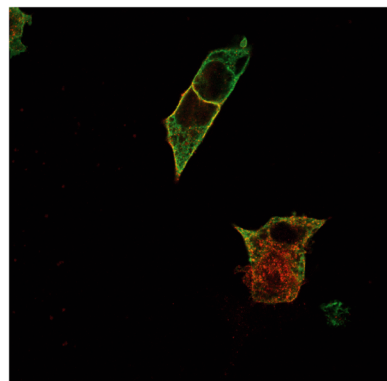
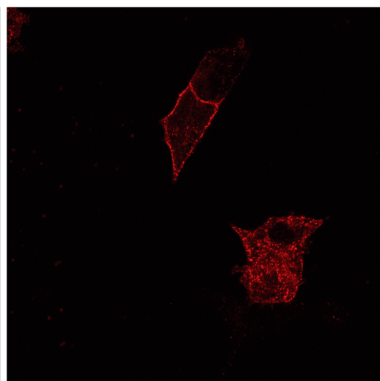
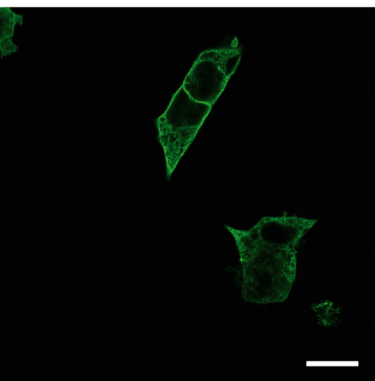
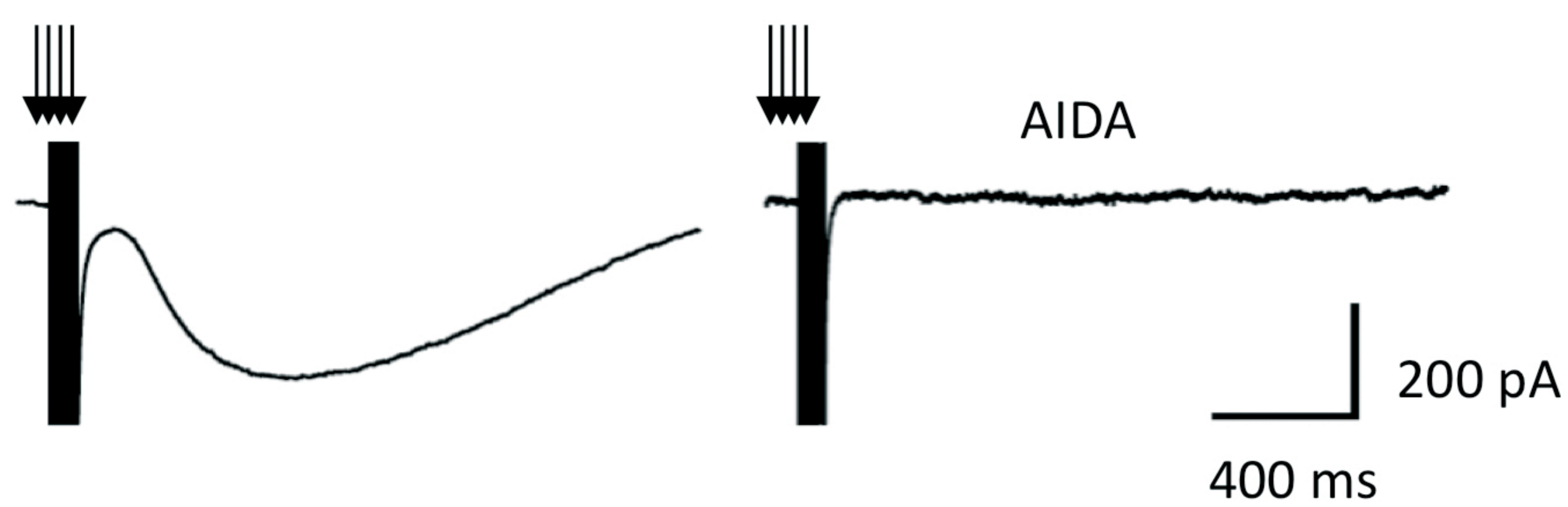
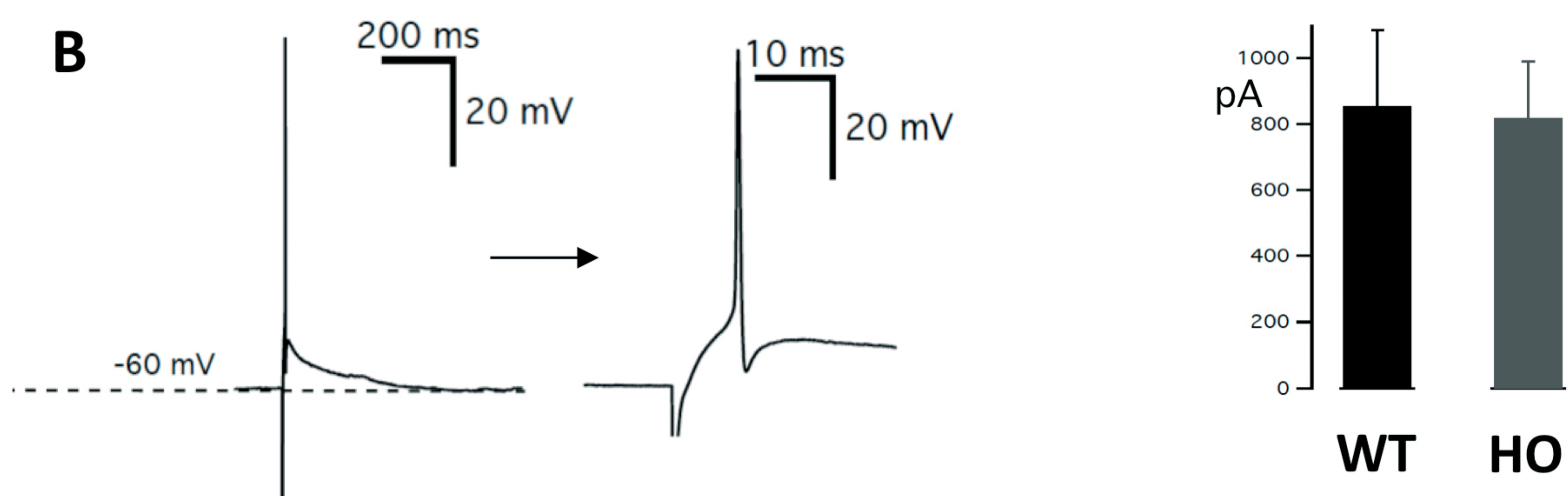


Figure S4

**A**



**B**



**C**

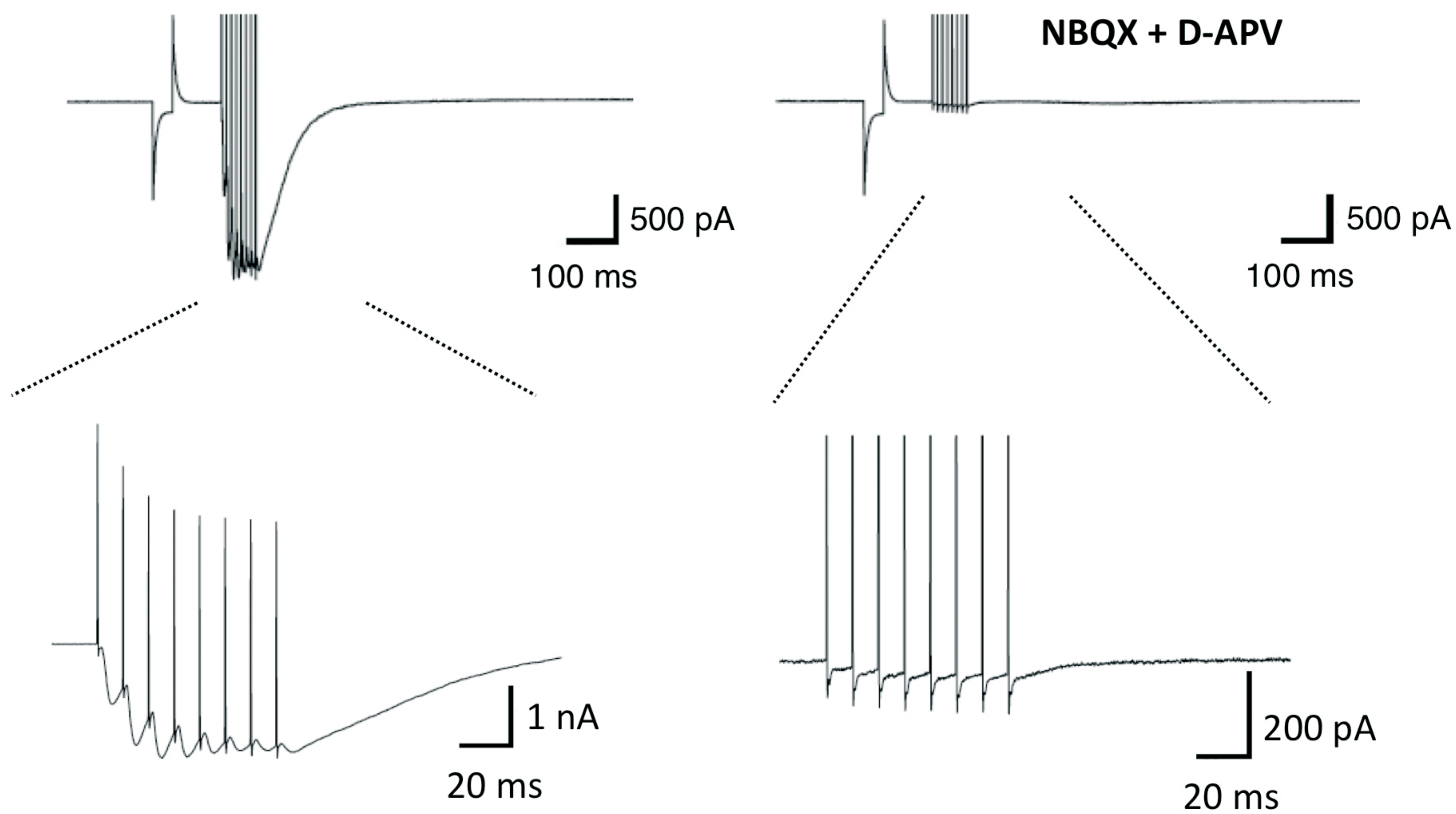


Figure S5

